Commun. Theor. Phys. **73** (2021) 035002 (9pp) https://doi.org/10.1088/1572-9494/abd84a

Editor's Suggestion

Modeling the COVID-19 epidemic and awareness diffusion on multiplex networks

Le He and Linhe Zhu*

School of Mathematical Sciences, Jiangsu University, Zhenjiang, 212013, China

E-mail: zlhnuaa@126.com

Received 17 September 2020, revised 16 December 2020
Accepted for publication 24 December 2020
Published 8 February 2021

Abstract

The coronavirus disease 2019 (COVID-19) has been widely spread around the world, and the control and behavior dynamics are still one of the important research directions in the world. Based on the characteristics of COVID-19's spread, a coupled disease-awareness model on multiplex networks is proposed in this paper to study and simulate the interaction between the spreading behavior of COVID-19 and related information. In the layer of epidemic spreading, the nodes can be divided into five categories, where the topology of the network represents the physical contact relationship of the population. The topological structure of the upper network shows the information interaction among the nodes, which can be divided into aware and unaware states. Awareness will make people play a positive role in preventing the epidemic diffusion, influencing the spread of the disease. Based on the above model, we have established the state transition equation through the microscopic Markov chain approach (MMCA), and proposed the propagation threshold calculation method under the epidemic model. Furthermore, MMCA iteration and the Monte Carlo method are simulated on the static network and dynamic network, respectively. The current results will be beneficial to the study of COVID-19, and propose a more rational and effective model for future research on epidemics.

Keywords: COVID-19, Multiplex network, Awareness spread, Propagation threshold

1. Introduction

The global spread of COVID-19, in which the outbreak began at the end of 2019, has had a huge impact on the world economy and human safety. The WHO report shows that the global mortality rate for COVID-19 is about 6.4%. Although the epidemic has been effectively controlled in some areas, the global epidemic situation is still very serious. Reasonable and effective mathematical modeling can provide great help to the government in anti-epidemic decision-making, disease prevention and control. Many researchers have established the spreading model of COVID-19 based on the traditional cabin model. Among them, some dynamics models have modified the traditional susceptible-infected-exposed-recovered (SIER) model and calculated the basic reproduction number [1–4]. Wu considered the impact of intercity traffic flow on disease transmission in the COVID-19 epidemic model and used the confirmed data of each city for comprehensive analysis [1]. Tang introduced the isolation and medical tracking mechanism to control the development of the epidemic [2]. Suwardi predicted that the emergence of vaccines would greatly accelerate the end of the epidemic [3]. Apart from the cabin classification of SIER models, some new methods of state classification have been proposed to better conform to the actual situation. In Chen's study [5], individuals could also be in a state of diagnosis and isolation, or death. At the same time, their model considered the phenomenon of delay in transfer between different states and the effect of taking isolation measures on the epidemic situation. With the intensifying of the epidemic research, it is further found that there may be asymptomatic patients during the spread of the new crown epidemic. In the study of Sun [6], individuals could be in one of the following five states: susceptible (S), asymptomatic (A), close observed (C), infected (I) and recovered (R). Based on these five states, a homogeneous mixed differential equation

* Author to whom any correspondence should be addressed.

model was established. Further, the model fitted the epidemic situation of specific cities and reveals the great influence of 'escapers' on disease spreading. In summary, the presentation of these models, all contribute to the prediction and control of COVID-19 propagation.

In recent years, the dynamics on the network have been developing continuously, which provides a new perspective for people to understand and study the spreading mechanism of infectious diseases. Because the relevant information is often closely related to the propagation behavior, the two-layer multiplex network model based on the dissemination mechanism of relevant information has begun to be applied in various dynamic modeling processes, such as epidemic propagation [7–16], rumor propagation [17, 18], multiplex information propagation [19–21], risk propagation [22, 27], behaviour progation [23] and so on. Granell divided the population of information diffusion process into two categories, namely the unaware (U) state and aware (A) state, and established a two-layer multiplex network model based on the traditional susceptible-infected-susceptible (SIS) model [7]. The model revealed the coupling effect of disease-related information and disease transmission. The effect of the information transmission network on the disease propagation threshold was further quantified. Moreover, Xia established a UAU-SIR model to represent the influence of relevant information on the traditional SIR model, and derived the epidemic threshold of disease transmission, which was proved to be related to the topology of the multiplex network and the coupling relationship between the two propagation dynamics [8]. Along these lines, they introduced the influence of the mass media in the later UAU-SIR model, and quantified the significant role of the mass media in inhibiting the spread of infectious diseases [9]. Zhu introduced the individual death state based on the UAU-SIR model, and then established a susceptible-infected-recovered-dead (UAU-SIRD) model [12]. They explained that the addition of an information layer had a significant impact on the range of disease transmission and the number of deaths.

Regardless, the above mathematical models provide valuable clues for us to describe and study the spreading behavior of an epidemic. However, for the study of COVID-19, many models are based on the hypothesis of uniform mixing of people, without considering the actual influence of the differences in contact patterns between different individuals on the spread of disease. Meanwhile, these models have ignored the influence of COVID-19-related information diffusion on the spreading behavior of the disease. Therefore, based on Sun's work [9], we can use the framework of the two-layer multiplex network to establish a COVID-19 disease-information coupling model, where the upper network is an unaware-aware-unaware (UWU) model. By improving the model, we will study the coupling dynamics of disease-information diffusion in a double-layer network structure. In previous work, during the process of establishing a multiplex network model, the disease contagion layer often depends on a relatively simple SIS or SIR model, so the threshold analysis generally involves only one infection cabin. However, in our work, the mechanism of disease spreading is established by the spread characteristics of COVID-19, in which the process of state transition is more complex, and the threshold analysis also involves multiple infection cabins.

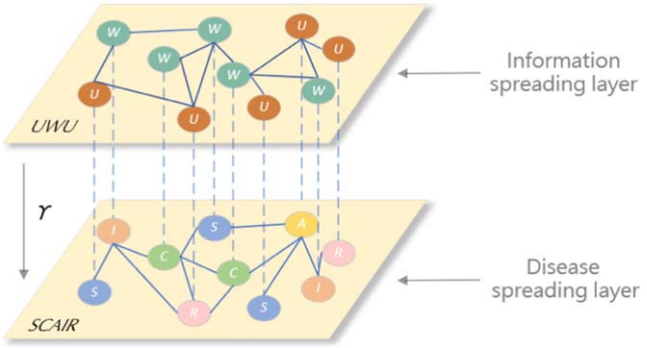

Figure 1. The multiplex network model.

The following structure of this paper is as follows: in the second section, we describe the basic structure of the double-layer multiplex network model, including the dynamic behavior of information and disease spreading in the upper and lower layers. Next, in the third section, the state transition probability tree and state transition equation of the model are established using the microscopic Markov chain approach (MMCA) method. In the fourth section, we simulate the model numerically. Finally, we put forward the conclusion of this paper in the fifth section.

2. Modeling

2.1. The spreading dynamics on each layer

As shown in figure 1, a two-layer multiplex network model is established to study the transmission process of COVID-19 with the influence of consciousness transmission. The upper network of the model represents the information layer, reflecting the status of different individuals' recognition and transmission of disease information. Among them, the nodes represent individuals, and edges represent the information interaction between nodes. People can spread information related to disease prevention in the information network. The lower network of the model represents the disease transmission layer, reflecting the status of different individuals and the transmission of infectious diseases. Among them, the nodes correspond to nodes in the upper network one to one, and connecting edges represent the actual contact between individuals. The state of each node is determined by the dynamic evolution of the upper and lower layers of the network. For the convenience of analysis and processing, it is assumed that the connecting edge structure of the two-layer network is independent, and the network is not directional.

Similar to the previous work [8, 9], we use the UWU model to describe the spreading process of disease awareness in the upper network. After a disease outbreak, an individual may be in an aware state (W) or unaware state (U). When an unaware person has a neighbor that is an aware person, the neighbor spreads the information about the disease to him,

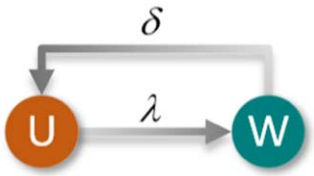

Figure 2. A description of the information spreading.

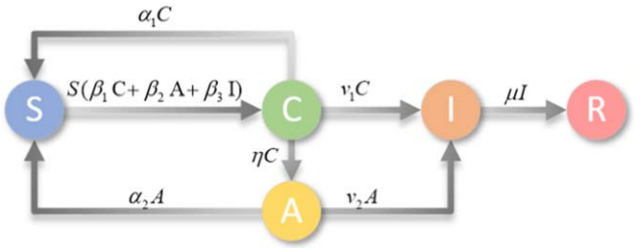

Figure 3. A description of the disease spreading.

making the unaware individual become aware at the probability of λ. At the same time, people's awareness of disease prevention will fade as time goes on, and in unit time, the aware will become unaware again with a probability of δ, as shown in figure 2.

The underlying network of the model is the disease spreading network. Based on Sun's work [6], we divide the population under the COVID-19 spreading network into five categories: susceptible (S), asymptomatic (A), close observed (C), infected (I) and recovered (R). If one is in the susceptible state, he may contact with close observed, infected and asymptomatic neighbors with a probability of β_1, β_2 and β_3, respectively, and will turn into the close observed state after contact. A close observed individual is going to change into an infected state or asymptomatic state with a probability of v_1 and η; meanwhile, he is going to release with a certain probability of α_1 going back to S. Asymptomatic patients will be diagnosed and turn into an infected state at the probability of v_2, and return to the susceptible state at the self-healing rate of α_2. Finally, the infected individual has a cure rate of μ to become recovered, as shown in figure 3.

2.2. Coupling propagation behavior on multiplex networks

Based on the above description, any individual can be in one of the following ten states: unaware–susceptible (US), aware–susceptible (WS), unaware–close observed (UC), aware–close observed (WC), unaware–asymptomatic (UA), aware–asymptomatic (WA), unaware–infected (UI), aware–infected (WI), unaware–recovered (UR), aware–recovered (WR). In fact, the propagation behavior of the upper and lower layers of the network is not independent, and the interaction of the propagation of the two layers of the network can be written as follows.

- When a susceptible individual in the network of disease spreading is in a state of awareness, he will take some measures to prevent disease. So, in the process of disease spreading, the aware will have a lower rate of β_s^{W} with others compared with an unaware contact rate of β_s^{U}, namely the $\beta_s^{\mathrm{W}} = \gamma\beta_s^{\mathrm{U}}$. Here, γ belongs to [0, 1], $s = 1, 2, 3$, where γ represents the prevention rate, which shows the influence of the upper network on the lower network.
- When an individual in a disease spreading network becomes close observed or infected, he becomes aware, regardless of whether the individual was previously aware or not. This is realistic because people in both states must already have received information about the spread of the disease. This connection can show the influence of the lower network on the upper network. Therefore, UC and UI are ignored in the subsequent analysis.

After explaining the above two links, any individual can only be in one of the following eight states: US, WS, WC, UA, WA, WI, UR, WR. The influence of the upper layer on the lower layer can adjust by γ. When $\gamma = 1$, it shows that the upper network has no impact on the underlying network; that is, the spreading of COVID-19 is independent of the diffusion of related information.

3. MMCA theoretical analysis

3.1. Probability tree and transition equation

In this section, based on the MMCA method, we will build the dynamical equation of eight possible states for the UWU-SCAIR model. At some point t, any individual can only be in one of the eight states, and the probability that node i is in various states at time t is denoted as $p_i^{\mathrm{US}}(t)$, $p_i^{\mathrm{WS}}(t)$, $p_i^{\mathrm{WC}}(t)$, $p_i^{\mathrm{UA}}(t)$, $p_i^{\mathrm{WA}}(t)$, $p_i^{\mathrm{WI}}(t)$, $p_i^{\mathrm{UR}}(t)$ and $p_i^{\mathrm{WR}}(t)$. With regard to the upper network, its adjacency matrix is denoted as $A = (a_{ij})$. Then, in the process of consciousness propagation, the probability that node i is not propagated by j in unit time can be expressed as

$$r_i(t) = \prod_j [1 - a_{ij} P_j^{\mathrm{W}}(t)\lambda]. \tag{3.1}$$

Similarly, the adjacency matrix of the lower network is denoted as $B = (b_{ij})$. If node j is a neighbor of i, then the probability that node j makes i turn to the close observed state from the susceptible state can be expressed as $P_j^{\mathrm{C}}(t)\beta_1^{\mathrm{U}} + P_j^{\mathrm{A}}(t)\beta_2^{\mathrm{U}} + P_j^{\mathrm{I}}(t)\beta_3^{\mathrm{U}}$. Further, we represent the probability that US does not convert to C as $q_i^{\mathrm{U}}(t)$, and the probability that WS does not convert to C as $q_i^{\mathrm{W}}(t)$. Then, the following equation can be obtained

$$\begin{cases} q_i^{\mathrm{U}}(t) = \prod_j [1 - b_{ij}(P_j^{\mathrm{C}}(t)\beta_1^{\mathrm{U}} + P_j^{\mathrm{A}}(t)\beta_2^{\mathrm{U}} + P_j^{\mathrm{I}}(t)\beta_3^{\mathrm{U}})], \\ q_i^{\mathrm{W}}(t) = \prod_j [1 - b_{ij}(P_j^{\mathrm{C}}(t)\beta_1^{\mathrm{W}} + P_j^{\mathrm{A}}(t)\beta_2^{\mathrm{W}} + P_j^{\mathrm{I}}(t)\beta_3^{\mathrm{W}})], \end{cases} \tag{3.2}$$

where $P_j^{\mathrm{C}}(t) = P_j^{\mathrm{WC}}(t)$, $P_j^{\mathrm{A}}(t) = P_j^{\mathrm{UA}}(t) + P_j^{\mathrm{WA}}(t)$, $P_j^{\mathrm{I}}(t) = P_j^{\mathrm{WI}}(t)$.

So far, we have obtained the transition probability tree of eight states, as shown in figure 4. Then, according to the probability tree in figure 4, we establish the dynamic evolution equation of eight possible states using the MMCA method, as

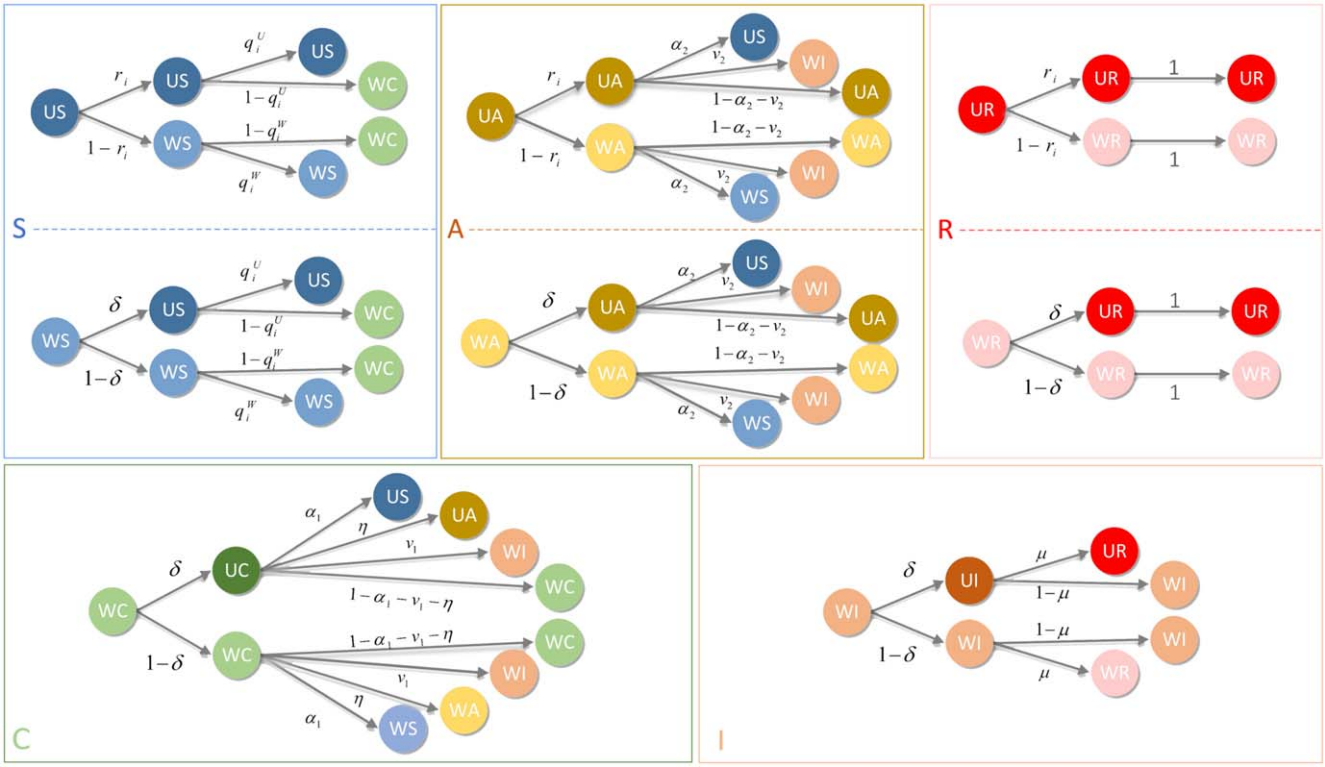

Figure 4. The probability trees for eight states.

shown below.

$$\begin{cases} P_i^{\mathrm{US}}(t+1) &= P_i^{\mathrm{US}}(t) r_i q_i^{\mathrm{U}} + P_i^{\mathrm{WS}}(t)\delta q_i^{\mathrm{U}} + P_i^{\mathrm{UA}}(t) r_i \alpha_2 \\ &\quad + P_i^{\mathrm{WA}}(t)\delta\alpha_2 + P_i^{\mathrm{WC}}(t)\delta\alpha_1, \\ P_i^{\mathrm{WS}}(t+1) &= P_i^{\mathrm{US}}(t)(1-r_i) q_i^{\mathrm{W}} + P_i^{\mathrm{WS}}(t)(1-\delta) q_i^{\mathrm{W}} \\ &\quad + P_i^{\mathrm{UA}}(t)(1-r_i)\alpha_2 + P_i^{\mathrm{WA}}(t)(1-\delta)\alpha_2 \\ &\quad + P_i^{\mathrm{WC}}(t)(1-\delta)\alpha_1, \\ P_i^{\mathrm{UA}}(t+1) &= P_i^{\mathrm{UA}}(t) r_i (1-v_2-\alpha_2) \\ &\quad + P_i^{\mathrm{WA}}(t)\delta(1-v_2-\alpha_2) \\ &\quad + P_i^{\mathrm{WC}}(t)\delta\eta, \\ P_i^{\mathrm{WA}}(t+1) &= P_i^{\mathrm{UA}}(t)(1-r_i)(1-v_2-\alpha_2) \\ &\quad + P_i^{\mathrm{WA}}(t)(1-\delta)(1-v_2-\alpha_2) \\ &\quad + P_i^{\mathrm{WC}}(t)(1-\delta)\eta, \\ P_i^{\mathrm{WC}}(t+1) &= P_i^{\mathrm{WC}}(t)(1-\alpha_1-v_1-\eta) \\ &\quad + P_i^{\mathrm{US}}(t)[r_i(1-q_i^{\mathrm{U}}) + (1-r_i)(1-q_i^{\mathrm{W}})] \\ &\quad + P_i^{\mathrm{WS}}(t)[\delta(1-q_i^{\mathrm{U}}) + (1-\delta)(1-q_i^{\mathrm{W}})], \\ P_i^{\mathrm{WI}}(t+1) &= P_i^{\mathrm{WI}}(t)(1-\mu) + P_i^{\mathrm{UA}}(t) v_2 + P_i^{\mathrm{WA}}(t) v_2 \\ &\quad + P_i^{\mathrm{WC}}(t) v_1, \\ P_i^{\mathrm{UR}}(t+1) &= P_i^{\mathrm{UR}}(t) r_i + P_i^{\mathrm{WR}}(t)\delta + P_i^{\mathrm{WI}}(t)\delta\mu, \\ P_i^{\mathrm{WR}}(t+1) &= P_i^{\mathrm{UR}}(t)(1-r_i) + P_i^{\mathrm{WR}}(t)(1-\delta) \\ &\quad + P_i^{\mathrm{WI}}(t)(1-\delta)\mu. \end{cases} \tag{3.3}$$

The first expression indicates that node i at time t has a certain probability to be converted into US at the next time step $t+1$ under US, WS, UA, WA and WC. Other equations also have similar meanings.

3.2. Threshold analysis

The epidemic threshold is an important value in the study of epidemic dynamics. We can solve the epidemic threshold using the above MMCA model. Around the threshold, the probability of any individual being infected approaches zero, and we can assume that $P_i^{\mathrm{C}} = P_i^{\mathrm{WC}} = \varepsilon_i^{\mathrm{C}} \ll 1$, $P_i^{\mathrm{I}} = P_i^{\mathrm{WI}} = \varepsilon_i^{\mathrm{I}} \ll 1$, $P_i^{\mathrm{A}} = P_i^{\mathrm{UA}} + P_i^{\mathrm{WA}} = \varepsilon_i^{\mathrm{UA}} + \varepsilon_i^{\mathrm{WA}} = \varepsilon_i^{\mathrm{A}} \ll 1$. Thus, by ignoring the higher-order term of $\varepsilon_i^{\mathrm{C}}$, $\varepsilon_i^{\mathrm{I}}$ and $\varepsilon_i^{\mathrm{A}}$, then $q_i^{\mathrm{U}}(t)$ and $q_i^{\mathrm{W}}(t)$ can be simplified as follows

$$\begin{cases} q_i^{\mathrm{U}}(t) &= \prod_j [1 - b_{ij}(P_j^{\mathrm{C}}(t)\beta_1^{\mathrm{U}} + P_j^{\mathrm{A}}(t)\beta_2^{\mathrm{U}} + P_j^{\mathrm{I}}(t)\beta_3^{\mathrm{U}})] \\ &\approx 1 - \sum_j b_{ij}(\beta_1^{\mathrm{U}}\varepsilon_j^{\mathrm{C}} + \beta_2^{\mathrm{U}}\varepsilon_j^{\mathrm{A}} + \beta_3^{\mathrm{U}}\varepsilon_j^{\mathrm{I}}), \\ q_i^{\mathrm{W}}(t) &= \prod_j [1 - b_{ij}(P_j^{\mathrm{C}}(t)\beta_1^{\mathrm{W}} + P_j^{\mathrm{A}}(t)\beta_2^{\mathrm{W}} + P_j^{\mathrm{I}}(t)\beta_3^{\mathrm{W}})] \\ &\approx 1 - \sum_j b_{ij}(\beta_1^{\mathrm{W}}\varepsilon_j^{\mathrm{C}} + \beta_2^{\mathrm{W}}\varepsilon_j^{\mathrm{A}} + \beta_3^{\mathrm{W}}\varepsilon_j^{\mathrm{I}}). \end{cases} \tag{3.4}$$

Let $\sigma_i^{\mathrm{U}} = \sum_j b_{ij}(\beta_1^{\mathrm{U}}\varepsilon_j^{\mathrm{C}} + \beta_2^{\mathrm{U}}\varepsilon_j^{\mathrm{A}} + \beta_3^{\mathrm{U}}\varepsilon_j^{\mathrm{I}})$, $\sigma_i^{\mathrm{W}} = \sum_j b_{ij}(\beta_1^{\mathrm{W}}\varepsilon_j^{\mathrm{C}} + \beta_2^{\mathrm{W}}\varepsilon_j^{\mathrm{A}} + \beta_3^{\mathrm{W}}\varepsilon_j^{\mathrm{I}})$. Through the above formula, the equations of US, WS and WC in equation (3.3) can be rewritten into the

following formula

$$P_i^{\mathrm{US}}(t+1) = P_i^{\mathrm{US}}(t) r_i (1-\sigma_i^{\mathrm{U}}) + P_i^{\mathrm{WS}}(t)\delta(1-\sigma_i^{\mathrm{U}}) + P_i^{\mathrm{UA}}(t) r_i \alpha_2 + P_i^{\mathrm{WA}}(t)\delta\alpha_2 + P_i^{\mathrm{WC}}(t)\delta\alpha_1, \tag{3.5a}$$

$$P_i^{\mathrm{WS}}(t+1) = P_i^{\mathrm{US}}(t)(1-r_i)(1-\sigma_i^{\mathrm{W}}) + P_i^{\mathrm{WS}}(t)(1-\delta)(1-\sigma_i^{\mathrm{W}}) + P_i^{\mathrm{UA}}(t)(1-r_i)\alpha_2 + P_i^{\mathrm{WA}}(t)(1-\delta)\alpha_2 + P_i^{\mathrm{WC}}(t)(1-\delta)\alpha_1, \tag{3.5b}$$

$$P_i^{\mathrm{WC}}(t+1) = P_i^{\mathrm{WC}}(t)(1-\alpha_1-\nu_1-\eta) + P_i^{\mathrm{US}}(t)[r_i\sigma_i^{\mathrm{U}} + (1-r_i)\sigma_i^{\mathrm{W}}] + P_i^{\mathrm{WS}}(t)[\delta\sigma_i^{\mathrm{U}} + (1-\delta)\sigma_i^{\mathrm{W}}]. \tag{3.5c}$$

When $t \to \infty$, the system tends to approach the stationary state. We can assume that $P_i(t+1) = P_i(t)$. The equation of US, WS in equation (5) can be further reduced into the following relationship by assuming $\varepsilon \to 0$:

$$\begin{cases} P_i^{\mathrm{US}} = P_i^{\mathrm{US}} r_i + P_i^{\mathrm{WS}}\delta, \\ P_i^{\mathrm{WS}} = P_i^{\mathrm{US}}(1-r_i) + P_i^{\mathrm{WS}}(1-\delta). \end{cases} \tag{3.6}$$

When $t \to \infty$, the equations of WC in equation (5) and UA, WA, WI in equation (3.3) can be written as

$$\begin{cases} \varepsilon_i^{\mathrm{UA}} = (\varepsilon_i^{\mathrm{UA}} r_i + \varepsilon_i^{WA}\delta)(1-\nu_2-\alpha_2) + \varepsilon_i^{\mathrm{C}}\delta\eta, \\ \varepsilon_i^{\mathrm{WA}} = \varepsilon_i^{\mathrm{UA}}(1-r_i)(1-\nu_2-\alpha_2) + \varepsilon_i^{\mathrm{WA}}(1-\delta)(1-\nu_2-\alpha_2) + \varepsilon_i^{\mathrm{C}}(1-\delta)\eta, \\ \varepsilon_i^{\mathrm{C}} = \varepsilon_i^{\mathrm{C}}(1-\alpha_1-\nu_1-\eta) + P_i^{\mathrm{US}}[r_i\sigma_i^{\mathrm{U}} + (1-r_i)\sigma_i^{\mathrm{W}}] + P_i^{\mathrm{WS}}[\delta\sigma_i^{\mathrm{U}} + (1-\delta)\sigma_i^{\mathrm{W}}], \\ \varepsilon_i^{\mathrm{I}} = \varepsilon_i^{\mathrm{I}}(1-\mu) + \varepsilon_i^{\mathrm{UA}}\nu_2 + \varepsilon_i^{\mathrm{WA}}\nu_2 + \varepsilon_i^{\mathrm{C}}\nu_1. \end{cases} \tag{3.7}$$

Equation (3.7) can be further simplified as

$$\begin{aligned} \alpha_2\varepsilon_i^{\mathrm{A}} + \alpha_1\varepsilon_i^{\mathrm{C}} + \mu\varepsilon_i^{\mathrm{I}} &= \sigma_i^{\mathrm{U}}(P_i^{\mathrm{US}} r_i + P_i^{\mathrm{WS}}\delta) + \sigma_i^{\mathrm{W}}[P_i^{\mathrm{US}}(1-r_i) + P_i^{\mathrm{WS}}(1-\delta)] \\ &= \sigma_i^{\mathrm{U}} P_i^{\mathrm{US}} + \sigma_i^{\mathrm{W}} P_i^{\mathrm{WS}} \\ &= \sigma_i^{\mathrm{U}}(P_i^{\mathrm{US}} + \gamma P_i^{\mathrm{WS}}). \end{aligned} \tag{3.8}$$

Let $\varepsilon_i^{\mathrm{C}} = k_1\varepsilon_i^{\mathrm{I}}$ and $\varepsilon_i^{\mathrm{A}} = k_2\varepsilon_i^{\mathrm{I}}$. Furthermore, let $P_i^{\mathrm{W}} = P_i^{\mathrm{WS}} + P_i^{\mathrm{WC}} + P_i^{\mathrm{WA}} + P_i^{\mathrm{WI}} + P_i^{\mathrm{WR}}$. Near the epidemic threshold, $P_i^{\mathrm{WR}} \to 0$, $P_i^{\mathrm{WC}} \to 0$, $P_i^{\mathrm{WA}} \to 0$, $P_i^{\mathrm{WI}} \to 0$, provided that the initial fraction of susceptible agents is the vast majority. Hence, we assume $P_i^{\mathrm{W}} \approx P_i^{\mathrm{WS}}$, $P_i^{\mathrm{US}} \approx 1 - P_i^{\mathrm{W}}$ and the equation of equation (3.8) can be further simplified as

$$\sum_j [(1-(1-\gamma)P_i^{\mathrm{W}})b_{ij} - \frac{\alpha}{\beta}e_{ij}]\varepsilon_j^{\mathrm{I}} = 0, \tag{3.9}$$

where $\alpha = \mu + \alpha_2 k_2 + \alpha_1 k_1$, $\beta = \beta_1^{\mathrm{U}} k_1 + \beta_2^{\mathrm{U}} k_2 + \beta_3^{\mathrm{U}}$, and e_{ij} represents the member of the identity matrix. Thus, the critical threshold can be considered as the solution of the maximum eigenvalue problem of H, whose elements are $h_{ij} = (1-(1-\gamma)P_i^{\mathrm{W}})b_{ij}$. Then, the epidemic threshold regarding the current two-layered model can be described as follows

$$\beta_c = (\beta_1^{\mathrm{U}} k_1 + \beta_2^{\mathrm{U}} k_2 + \beta_3^{\mathrm{U}})_c = \frac{\alpha}{\Lambda_{\max}(H)}. \tag{3.10}$$

When the value of $\beta_1^{\mathrm{U}} k_1 + \beta_2^{\mathrm{U}} k_2 + \beta_3^{\mathrm{U}}$ is greater than the threshold β_c, the disease will spread in the population. Otherwise, the disease cannot spread to a great fraction of the population. It is worth noting that λ and a_{ij} do not appear explicitly in equation (3.10), but the value of λ and the topological structure of the upper network will jointly affect the fraction of aware nodes. Thus, we presume that the above two parameters may affect the threshold [7].

4. Numerical simulations

4.1. Simulation results of static network

In this section, a coupled two-layer static network is established as the basis for numerical simulation of the UWU-SCAIR model, in which the upper network is a random Erdos–Renyi (ER) network with 1000 nodes with a connecting probability of 0.1, and the lower network is a Barabasi–Albert (BA) scale-free network with the power exponent of 3. Scale-free networks are highly heterogeneous and can describe the contact structure of people well. Then, the dynamic evolution of the UWU-SCAIR model in the above two-layer network will be simulated by an extensive MMCA iterative algorithm. The MMCA iterative algorithm is based on the state transfer process of the traditional non-homogeneous discrete Markov chain. At $t = 0$, we give the initial state distribution vector ($p_i^{\mathrm{US}}(0)$, $p_i^{\mathrm{WS}}(0)$, $p_i^{\mathrm{WC}}(0)$, $p_i^{\mathrm{UA}}(0)$, $p_i^{\mathrm{WA}}(0)$, $p_i^{\mathrm{WI}}(0)$, $p_i^{\mathrm{UR}}(0)$, $p_i^{\mathrm{WR}}(0)$) for any node i. With the help of the adjacent matrix of the two-layer network, the values of equation (3.1) and equation (3.2) at $t+1$ can be calculated for each node after the state distribution vector of each node is known at time t. Further, we can calculate the probability of each node in each state at time $t+1$ by equation (3.3), and update the state distribution vector.

First, in figure 5, we illustrate the variation of the proportion of recovered individuals (ρ^{R}) with λ and the contact rates β_1, β_2, β_3, where $\rho^{\mathrm{R}} = \sum_i P_i^{\mathrm{R}}(t=\infty)/N$, and N represents the total number of nodes presented in the system. The proportion of recovered individuals in the stationary state can characterize the number of nodes infected throughout the epidemic. The results show that the number of nodes affected by the epidemic is positively correlated with the contact rate, among which β_3 has the most influence, followed by β_2. When the contact rate is low, small changes will cause a large change in the spread of the epidemic. Meanwhile, the range of disease diffusion is negatively correlated with λ. Compared with the disease transmission layer, and independent of the information transmission layer, effective prevention of awareness transmission will play a very effective role in resisting infectious diseases.

It is worth mentioning that we also utilize the Monte Carlo method (MC) to run independently 50 times to get the

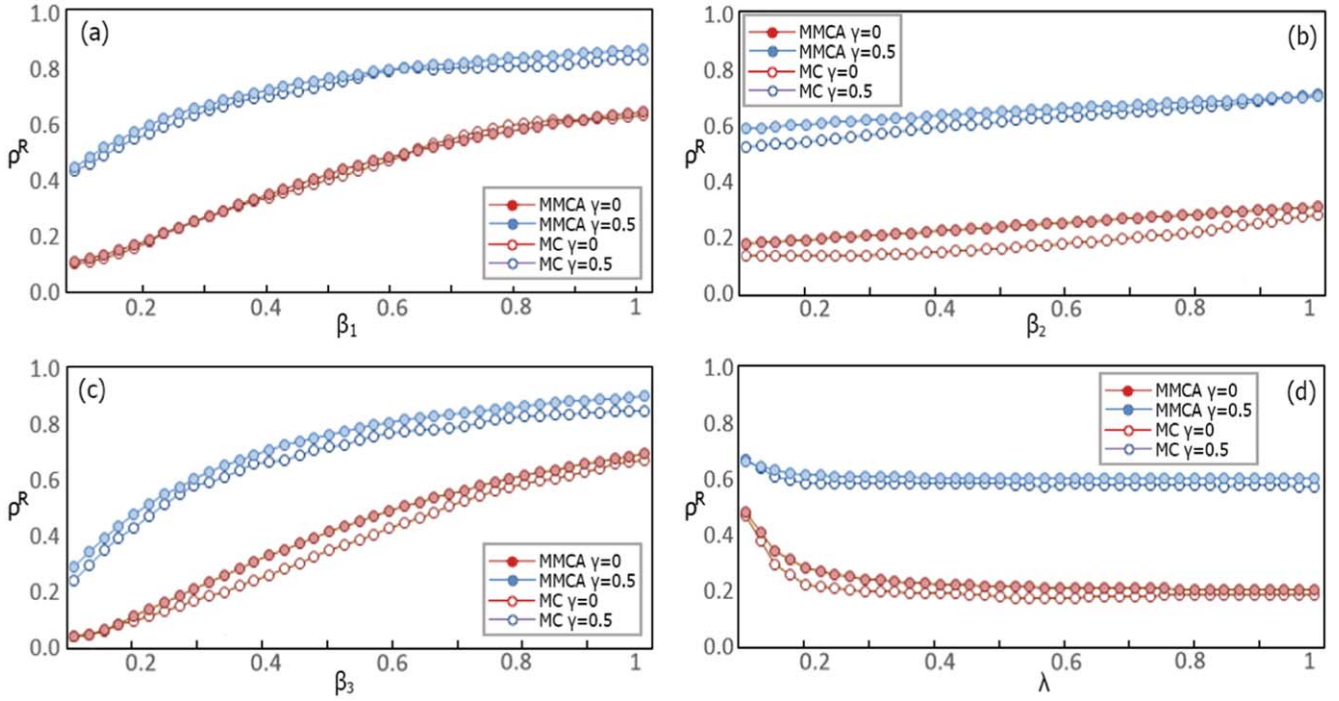

Figure 5. The ratio of the recovered (ρ^R) at the stationary state varies with the parameters β_1, β_2, β_3 and λ, based on the MMCA iteration method and the MC method. In panel (a), the red and blue curves represent $\gamma = 0$ and $\gamma = 0.5$, respectively, and the parameters β_2, β_3 and λ are set as 0.2, 0.25 and 0.5. In panel (b), the parameters β_1, β_3 and λ are set as 0.2, 0.25 and 0.5. In panel (c), the parameters β_1, β_2 and λ are set as 0.2, 0.2 and 0.5. In panel (d), the parameters β_1, β_2 and β_3 are set as 0.2, 0.2 and 0.25. Other parameters are set as follows: $\delta = 0.4$, $\alpha_1 = 0.2$, $\alpha_2 = 0.5$, $\eta = 0.1$, $v_1 = 0.4$, $v_2 = 0.1$, $\mu = 0.4$.

evolution results of the UWU-SCAIR in the two-layer network. The MC method can better reflect the evolution process of the model in the actual propagation process. We find that the results of the two methods are in good agreement, which indicates that the MMCA iterative algorithm can describe the actual propagation process very well. Although on the whole, the number of recovered nodes obtained by the MC method is slightly smaller than that of the MMCA iterative method. We will only consider the evolution process of the UWU-SCAIR model in the two-layer network based on the MMCA algorithm in the following work.

In the following, we further explore the relationship between ρ^{R} or the fraction of aware individuals at the steady state ($\rho^{\mathrm{W}} = \sum_i P_i^{\mathrm{W}}(t = \infty)/N$), and the awareness weakening rate δ at different awareness spreading rates λ in figure 6. With the increase in δ, because of the increasing conversion rate of unaware individuals from the aware state, ρ^{R} is higher and ρ^{W} is lower, but their rate of change will gradually decrease. Similar to the results in figure 5, when λ is higher, ρ^{R} is lower, and its effect on ρ^{R} is similar at different values of δ. Conversely, the increase in λ leads to lower ρ^{W}, which is in line with the reality, and the greater the value of δ, the greater the impact on ρ^{W}.

In figures 7 and 8, we investigate the effects of v_1 and v_2 on disease transmission at different values of μ and η. In panel (a) of figure 7, η is set at 0.1, at which point the closely observed individuals are more likely to become infected. At a low cure rate ($\mu = 0.2$), v_1 has a great positive correlation to ρ^{R}, while at a high cure rate ($\mu = 0.6$), the impact of v_1 on ρ^{R} is relatively less. Then, in panel (b) of figure 7, η is set at 0.4,

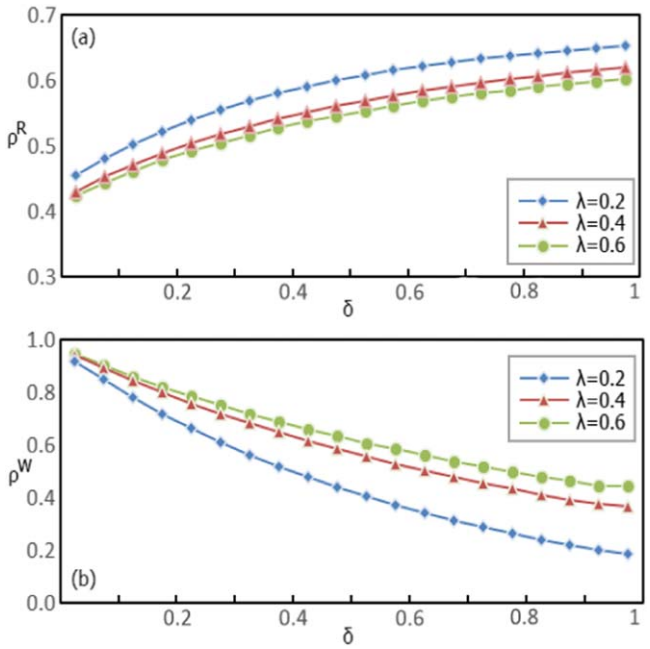

Figure 6. The ratio of the recovered (ρ^{R}) and the aware (ρ^{W}) at the stationary state varies with the parameters δ. The green, red and blue curves represent $\lambda = 0.6$, $\lambda = 0.4$ and $\lambda = 0.2$, respectively. Other parameters are set as follows: $\beta_1 = 0.2$, $\beta_2 = 0.2$, $\beta_3 = 0.25$, $\gamma = 0.5$, $\alpha_1 = 0.2$, $\alpha_2 = 0.5$, $\eta = 0.1$, $v_1 = 0.4$, $v_2 = 0.1$, $\mu = 0.4$.

and the probability of the closely observed state turning into the asymptomatic state increases, while the positive correlation of v_1 on ρ^{R} decreases.

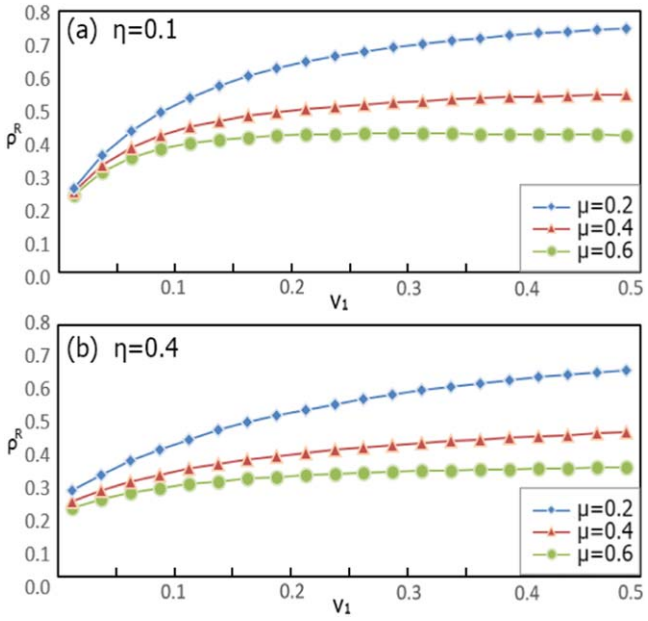

Figure 7. The ratio of the recovered (ρ^R) in the stationary state varies with the parameters v_1. In panel (a), the green, red and blue curves represent $\mu = 0.6$, $\mu = 0.4$ and $\mu = 0.2$, respectively, and the parameter η is set as 0.1. In panel (b), the parameter η is set as 0.4. Other parameters are set as follows: $\lambda = 0.5$, $\delta = 0.4$, $\beta_1 = 0.2$, $\beta_2 = 0.2$, $\beta_3 = 0.25$, $\gamma = 0.5$, $\alpha_1 = 0.2$, $\alpha_2 = 0.5$, $v_2 = 0.1$.

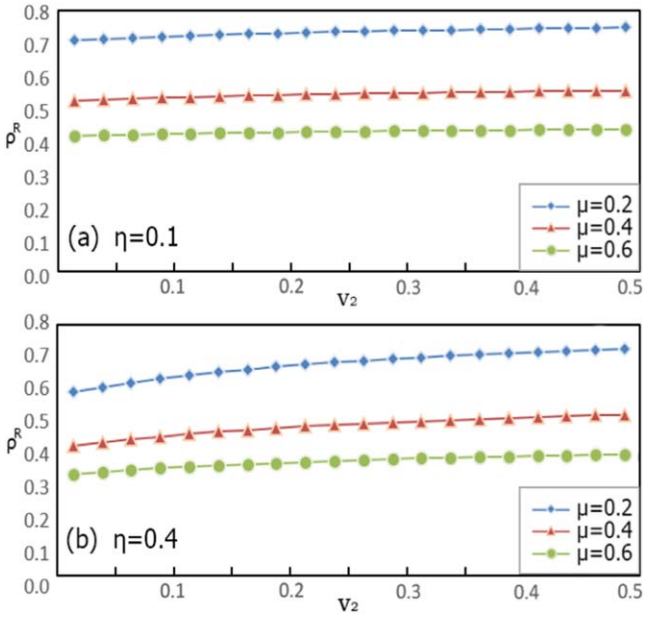

Figure 8. The ratio of the recovered (ρ^R) in the stationary state varies with the parameters v_2. In panel (a), the green, red and blue curves represent $\mu = 0.6$, $\mu = 0.4$ and $\mu = 0.2$, respectively, and the parameter η is set as 0.1. In panel (b), the parameter η is set as 0.4. Other parameters are set as follows: $\lambda = 0.5$, $\delta = 0.4$, $\beta_1 = 0.2$, $\beta_2 = 0.2$, $\beta_3 = 0.25$, $\gamma = 0.5$, $\alpha_1 = 0.2$, $\alpha_2 = 0.5$, $v_1 = 0.4$.

Similarly, in figure 8, we have investigated the effect of v_2 on disease transmission. Significantly different from v_1, although ρ^R also increases with the addition of v_2, its change is very gentle, and when the value of v_2 is very small, the effect of μ on ρ^R is still significant. From the above analysis, it can be judged that in the disease spreading system with current parameters, compared with asymptomatic patients, the effect of controlling the close observed population on the spread of the disease is more significant.

4.2. Simulation results of dynamic network

In this section, we establish a coupled dynamic double-layer network based on social responsibility and self-segregation, in which the evolution mechanism of the network is as follows.

- Because people's social networks present scale-free characteristics, in the initial state, we construct the upper network as a scale-free network with 1000 nodes and a power exponent of 2.5. The structure of the network is generated by the configuration model. At each time step, nodes in the aware state in the network have a probability of actively expanding their information exchange circle, trying to obtain more relevant information, or transmitting disease information to strangers out of a sense of social responsibility. At the same time, a new edge is established. It is reasonable to think that when a node has more neighbors, the stronger its sense of responsibility, the greater the probability of connecting edges. The maximum number of new connections in the network at one time step is τ_1, and the probability of $P_i^W(t)\frac{k_i(t)}{N\langle k(t)\rangle}$ for any new connections is initiated from the node i and connected to any non-neighbor node. After a time step, the total number of new connections in the network is $\sum_i P_i^W(t)\frac{k_i(t)}{N\langle k(t)\rangle}\tau_1$, where k_i represents the degree of i, and $\langle k\rangle$ represents the average degree of nodes.
- The lower layer is the spreading layer of disease, and the same as the previous simulation process, and the disease spreading network is still a BA scale-free network. During the spread of the epidemic, conscious individuals will isolate themselves, thus reducing or severing contact with their neighbors and causing the edge fracture. It is reasonable to think that the more neighbors a node has, the greater the probability that it will be far away from some of its neighbors. Suppose that after a time step, the maximum number of edges broken is τ_2, the probability of any broken edges is broken by the node i and is $P_i^W(t)\frac{k_i(t)}{N\langle k(t)\rangle}$; then, after a time step, the total number of connected edges reduced by the lower layer network is $\sum_i P_i^W(t)\frac{k_i(t)}{N\langle k(t)\rangle}\tau_2$.

The UWU-SCAIR model is numerically simulated on the above network by the MMCA iterative method. The variation of ρ^R with τ_1 and τ_2 is shown in figure 9. When λ is high ($\lambda = 0.5$), it can be seen from the vertical direction of the panel (b) of figure 9 that the influence of τ_1 on the spread range of the disease is very limited; that is, the change in the topology of the upper network has little effect on the spread of the disease. When λ is low ($\lambda = 0.1$), the effect of τ_1 on the spread range of the disease increases significantly. In the illustrated range, τ_1 can bring up to 0.15 numerical changes to ρ^R. Different from the edge-connected process on the upper network, the edge-breaking process in the disease transmission network has a

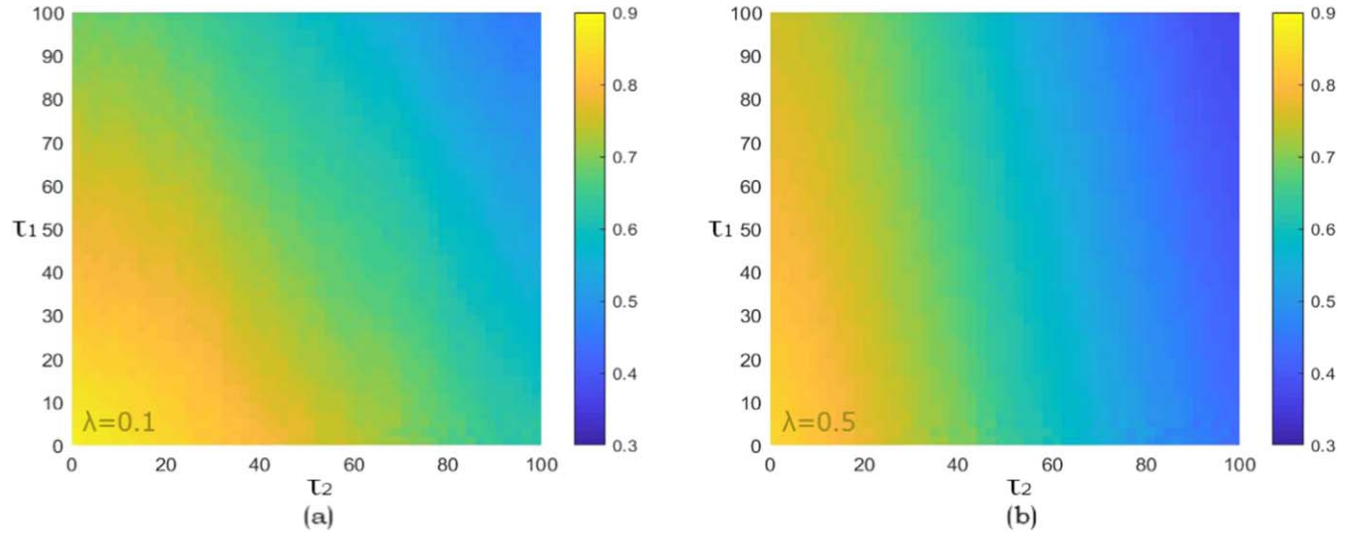

Figure 9. The ratio of the recovered (ρ^{R}) in the stationary state varies with the parameters τ_1, τ_2 in the two-layer dynamic network. In panel (a), the parameter λ is set as 0.1. In panel (b), the parameter λ is set as 0.5. Other parameters are set as follows: $\delta = 0.4$, $\beta_1 = 0.2$, $\beta_2 = 0.2$, $\beta_3 = 0.25$, $\gamma = 0.5$, $\alpha_1 = 0.2$, $\alpha_2 = 0.5$, $\nu_1 = 0.4$, $\nu_2 = 0.1$, $\mu = 0.4$.

great influence on the spread range of the disease. Here, τ_2 can reduce the ρ^{R} value by 0.4 in the graphical range under specific τ_1. It can be shown that self-segregation is a very effective way to resist infectious diseases.

5. Conclusions

Based on the propagation characteristics of the novel coronavirus, a coupled two-layer network UWU-SCAIR disease-information model is proposed to simulate and study the interaction and propagation behavior of the novel coronavirus and related awareness. In the lower layer of the disease transmission network, the population is divided into five categories, and the topology of the network shows the actual contact relationship of the population. The upper network represents the awareness propagation layer, and the crowd can only be in the aware or the unaware state. Based on the state classification of these two layers, any individual can be regarded as in one of the eight states. Further, based on the above model, we have established the transition probability tree and state transition equation of eight states using the MMCA method, and we calculated the propagation threshold of the epidemic model.

In addition, we perform the MMCA iteration and MC method on a two-layer static scale-free network, respectively, to simulate the model. The results show that the MMCA iterative method and MC method are very consistent, and the control of close observers can inhibit the spread of the disease more effectively than that of asymptomatic infected persons. Then, we build a two-layer dynamic network and use the MMCA iterative method to simulate the UWU-SCAIR model based on the network. The results show that self-segregation can effectively control the spread of infectious diseases. The current research will help to propose a more reasonable model for the transmission of new the coronavirus and future epidemiological research, and make more reasonable predictions and control efforts [24–26].

Acknowledgments

This research is supported by the National Natural Science Foundation of China (Grant No. 12002135), the Natural Science Foundation of Jiangsu Province (Grant No. BK20190836), China Postdoctoral Science Foundation (Grant No. 2019M661732), the Natural Science Research of Jiangsu Higher Education Institutions of China (Grant No. 19KJB110001) and Priority Academic Program Development of Jiangsu Higher Education Institutions (Grant No. PAPD-2018-87).

References

[1] Wu J T, Leung K and Leung G M 2020 Nowcasting and forecasting the potential domestic and international spread of the 2019-nCoV outbreak originating in Wuhan, China: a modelling study *Lancet* **395** 689–97
[2] Tang B, Wang X, Li Q, Bragazzi N L, Tang S Y, Xiao Y N and Wu J H 2020 Estimation of the transmission risk of the 2019-nCoV and its implication for public health interventions *J. Clin. Med.* **9** 462
[3] Annas S, Pratama M I, Rifandi M, Sanusi W and Side S 2020 Stability analysis and numerical simulation of SEIR model for pandemic COVID-19 spread in Indonesia *Chaos Solitons Fractals* **139** 110072
[4] He J Y, Chen G W, Jiang Y T, Jin R J, Shortridge A, Agusti S, He M J, Wu J P, Duarte C M and Christakos G 2020 Comparative infection modeling and control of COVID-19 transmission patterns in China, South Korea, Italy and Iran *Sci. Total Environ.* **747** 141447
[5] Chen Y, Cheng J, Jiang Y and Liu K J 2020 A time delay dynamical model for outbreak of 2019-nCoV and the parameter identification *J. Inverse Ill-Posed Problems* **28** 243–50

[6] Sun T Z and Wang Y 2020 Modeling COVID-19 epidemic in Heilongjiang province, China *Chaos Solitons Fractals* **138** 109949
[7] Granell C, Gomez S and Arenas A 2013 Dynamical interplay between awareness and epidemic spreading in multiplex networks *Phys. Rev. Lett.* **111** 128701
[8] Zheng C Y, Xia C Y, Guo Q T and Dehmer M 2018 Interplay between SIR-based disease spreading and awareness diffusion on multiplex networks *J. Parallel Distrib. Comput.* **115** 20–8
[9] Xia C Y, Wang Z S, Zheng C Y, Guo Q T, Shi Y T, Dehmer M and Chen Z Q 2019 A new coupled disease-awareness spreading model with mass media on multiplex networks *Inf. Sci.* **471** 185–200
[10] Wang Z S, Guo Q T, Sun S W and Xia C Y 2019 The impact of awareness diffusion on SIR-like epidemics in multiplex networks *Appl. Math. Comput.* **349** 134–47
[11] Granell C, Gomez S and Arenas A 2014 Competing spreading processes on multiplex networks: awareness and epidemics *Phys. Rev.* E **90** 012808
[12] Zhu P C, Wang X Y, Li S D, Guo Y M and Wang Z 2019 Investigation of epidemic spreading process on multiplex networks by incorporating fatal properties *Appl. Math. Comput.* **359** 512–24
[13] Yang J X 2018 Epidemic spreading in multiplex networks with heterogeneous infection rate *EPL* **124** 58004
[14] Ma Y F, Jiang X, Lei Y J, Li M, Ma Y F and Zheng Z M 2015 Two-stage effects of awareness cascade on epidemic spreading in multiplex networks *Phys. Rev.* E **91** 012822
[15] Zhu L H, Guan G and Li Y M 2019 Nonlinear dynamical analysis and control strategies of a network-based SIS epidemic model with time delay *Appl. Math. Modell.* **70** 512–31
[16] Miao P, Zhang Z D, Lim C W and Wang X D 2018 Hopf bifurcation and hybrid control of a delayed ecoepidemiological model with nonlinear incidence rate and Holling type II functional response *Math. Problems Eng.* **2018** 6052503
[17] Wang C X, Wang G S, Luo X P and Li H 2019 Modeling rumor propagation and mitigation across multiple social networks *Physica* A **535** 122240
[18] Zhu L H, Liu M X and Li Y M 2019 The dynamics analysis of a rumor propagation model in online social networks *Physica* A **520** 118–37
[19] Xiao Y P, Zhang L, Li Q and Liu L 2019 MM-SIS: Model for multiple information spreading in multiplex network *Physica* A **513** 135–46
[20] Li D D, Du J G, Sun M and Han D 2020 How conformity psychology and benefits affect individuals' green behaviours from the perspective of a complex network *J. Clean. Prod.* **248** 119215
[21] Li W Y, Tian L X, Gao X Y and Pan B R 2019 Impacts of information diffusion on green behavior spreading in multiplex networks *J. Clean. Prod.* **222** 488–98
[22] Liu H, Yang N D, Yang Z, Lin J H and Zhang Y L 2020 The impact of firm heterogeneity and awareness in modeling risk propagation on multiplex networks *Physica* A **539** 122919
[23] Gao X Y, Tian L X and Li W Y 2020 Coupling interaction impairs knowledge and green behavior diffusion in complex networks *J. Clean. Prod.* **249** 119419
[24] Hua J, An L X and Li Y M 2015 Bionic fuzzy sliding mode control and robustness analysis *Appl. Math. Modell.* **39** 4482–93
[25] Zhang F X, Hua J and Li Y M 2018 Indirect adaptive fuzzy control of SISO nonlinear systems with input-output nonlinear relationship *IEEE Trans. Fuzzy Syst.* **26** 2699–708
[26] Huo J W, Y M Li and Hua J 2019 Global dynamics of SIRS model with no full immunity on semidirected networks *Math. Problems Eng.* 8792497
[27] Huo L A, Guo H Y, Cheng Y Y and Xie X X 2020 A new model for supply chain risk propagation considering herd mentality and risk preference under warning information on multiplex networks *Physica* A **545** 123506